Research on Engineering Structures & Materials
www.jresm.org
MIM Research Group

Research Article

Performance of reinforced concrete two-way slabs incorporating recycled waste glass and hollow-tube reinforcement

Zeyad T. Ismael [*,a], Fadya S. Klak [b], Shareef S. Shareef [c]

College of Engineering, University of Tikrit, Tikrit, Iraq

Article Info

Article History:

Received 06 Aug 2026
Accepted 27 Oct 2026

Keywords:

Recycling;
Waste glass powder;
Hollow steel tubes;
Lightweight aggregate;
Two-way slabs

Abstract

This study experimentally investigates the structural performance of reinforced concrete two-way slabs, which are material-intensive floor elements, incorporating two recycled-material strategies. Thirteen slabs were tested in two groups. Group 1 comprised six 500 × 500 × 50 mm slabs, including a control (CS-GP0), in which waste glass powder replaced natural fine aggregate by weight at 0, 5, 10, 15, 20 and 25%. Group 2 comprised seven 650 × 1000 × 100 mm slabs, including two controls with ordinary steel reinforcement (CS-TH0-T0 with normal coarse aggregate and CS-TH50-T0 with 50% recycled Thermostone coarse aggregate), in which recycled hollow steel tubes replaced 20, 40, 60, 80 and 100% of the tensile reinforcement in slabs containing 50% Thermostone. All mixes targeted 30 MPa, verified on three cylinders per mix. Each slab was tested once to failure under a monotonic concentrated load at mid-span. Increasing the glass-powder content progressively reduced compressive strength and ultimate load; the 25% replacement lowered the ultimate load by about 32% relative to the control. Replacing the tensile reinforcement with hollow tubes progressively reduced the peak load from 37 kN for the control to 15 kN at 100% replacement (59%; 57% against the Thermostone reference), without a clear ductility-enhancing trend in the deflection at peak load. As each configuration had a single specimen, these trends are indicative rather than statistical. Glass powder should be limited to low replacement ratios, and the loss of capacity of tube-reinforced slabs must be considered in design; replicated testing is recommended before generalization.

© 2026 MIM Research Group. All rights reserved.

1. Introduction

Many necessary materials, like wood, naturally occurring stones, glass, and minerals, could cause significant harm to the environment and human health. Recycling these materials is fascinating from an economic and environmental standpoint. The two primary environmental concerns are either increasing the recycling of materials waste or utilizing them as additives with raw materials [1]. This will enable glass manufacturers, for example, to reduce their energy consumption and emissions of greenhouse gases [2]. In addition, eliminating glass waste by using it as aggregate in concrete will decrease the need for mineral aggregate in construction [3].

Nevertheless, using glass waste as aggregates may weaken alkali-concrete's mechanical qualities by expanding materials produced by silica reactions (ASR). Larger glass-cullet particle sizes were found to increase ASR expansion in concrete blocks, whereas incorporating pozzolanic materials substantially reduced it [4]. In the same aspect, a study by Prema Kumar et al. [5] found that partially replacing cement — not aggregate — with waste glass powder increased compressive and split-tensile strength up to an optimum replacement level of about 20%, beyond which strength

*Corresponding author: mr.ziadtariq@tu.edu.iq
[a]orcid.org/0000-0002-3827-5574; [b]orcid.org/0009-0007-5349-172X; [c]orcid.org/0009-0009-4973-9475
DOI: http://dx.doi.org/10.17515/resm2026-2119ma0806rs

declined. Also, Liaqat et al. [6] and Jomaa'h [7] found that the replacement of 20% glass waste and 25% Thermostone waste as coarse aggregate, with particle sizes of about 4.75–12.5 mm and different replacement ratios by weight, was the ideal amount for materials waste replacement, respectively. Conversely, Nwofor and Ukpaka [8] discovered that 20% was the perfect replacement for coarse and fine aggregates concerning the other percentages. Within the limits of particle sizes not exceeding 1.18 mm, Klak et al. [9] proved that using glass powder as a substitute for fine aggregate in concrete can reduce the amount of water absorbed by 25%, in addition to improving the appearance of the concrete.

The ongoing increase in cement and steel reinforcement costs leads people to find solutions to make concrete lighter. The weight impacts the construction project's overall cost and the environmental issues brought on by the massive use of steel and cement [10]. Several experiments concentrated on replacing steel bars with hollow steel pipes to lower the concrete bulk density. The hollow cores affect the reinforced concrete slabs' capacity to support loads, and it was found that this capacity insignificantly varies compared to slabs with ordinary reinforcement [11].

Another approach to decreasing the cost and weight of concrete is generating lightweight concrete (LWC), known for its thermal insulation, which reduces fire risks to structural elements [12]. It is crucial to reduce the range from around 300 to no more than 2000 kg/m3 [13]. Numerous studies that examined the structural behavior of manufactured lightweight concrete slabs have been presented in recent years [14–16]. This research aims to address the behavior of the reinforced concrete slabs constructed with recycled materials.

More recent studies have continued to reinforce the relevance of both material strategies adopted in this work. Mustafa et al. [17] reported that reinforced concrete beams containing recycled glass exhibited strength and serviceability behavior that remained within acceptable structural limits at moderate replacement ratios. Elsayed et al. [18] similarly found that combining waste glass powder with recycled coarse aggregate in reinforced beams altered flexural and shear performance in a predictable, quantifiable manner. Concerning the second strategy investigated here, Al-Bayati et al. [19] experimentally showed that one-way slabs containing longitudinal hollows suffered reductions in ultimate load and energy absorption that scaled with the hollow ratio, a trend consistent with the deflection and capacity behavior observed for the recycled-tube slabs in the present study. These recent contributions confirm that, despite growing interest in recycled-material slabs, experimental datasets combining both waste-glass fine aggregate and hollow-core tube reinforcement strategies within a single two-way slab investigation, as presented here, remain scarce. Two-way slabs were selected because they are among the most material-intensive floor elements in buildings, so any material-substitution strategy must be verified under biaxial flexure before it can be considered for practice. The objective of this study is therefore to evaluate experimentally the load-deflection response of two-way slabs incorporating (i) waste glass powder as a partial replacement of fine aggregate and (ii) recycled hollow steel tubes as a partial replacement of the tensile reinforcement in slabs containing Thermostone coarse aggregate, and to compare each against its control specimen.

Compared with the studies cited above, the present work differs in three respects: (i) the glass powder is assessed at slab level under biaxial flexure, rather than through material-level properties or beam tests; (ii) the replacement of tensile reinforcement by recycled hollow tubes is examined at five replacement ratios in slabs that also contain 50% recycled Thermostone aggregate; and (iii) both strategies are tested against their own control specimens within one experimental program, so that their effects on load capacity and deflection can be compared on a common basis.

2. Materials and Methods

2.1 Geometry of The Specimens

The specimens tested in this study consisted of two groups of slabs. The first group included six slabs with dimensions of 500 mm x 500 mm and a thickness of 50 mm, as illustrated in Figure 1. The first specimen served as the control, constructed without the inclusion of glass powder (GP). The remaining five slabs were fabricated with glass powder replacing the fine aggregate at 5%,

10%, 15%, 20%, and 25% by weight (mass) of the fine aggregate replaced, consistent with the kg/m^3 mix proportions given in Table 3; no specific-gravity volume correction was applied.

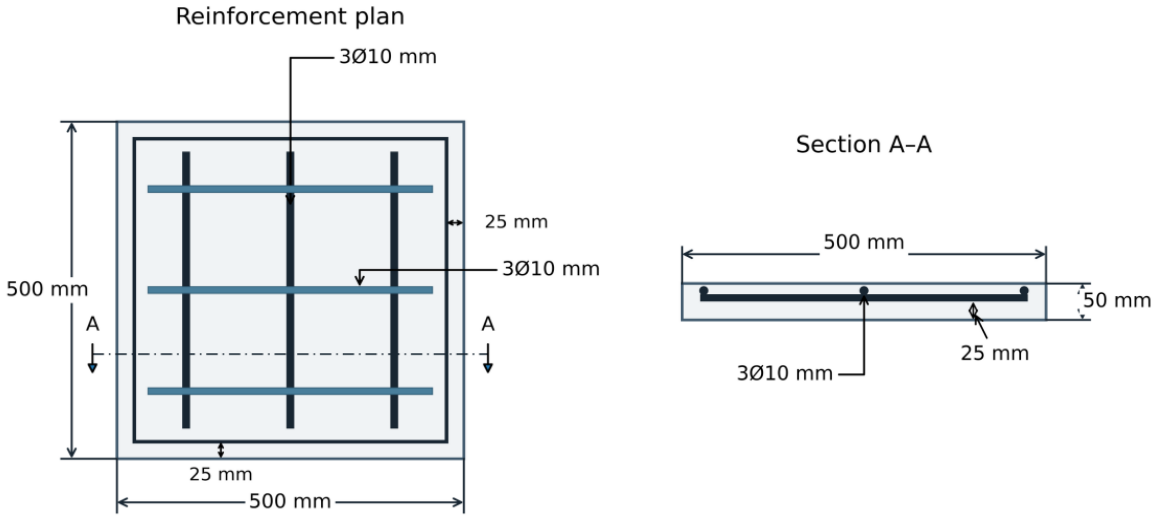


Fig. 1. Reinforcement details for the Group 1

For the first group of the slabs, the bottom longitudinal reinforcements (tensile steel reinforcement) consisted of Three Ø10 deformed steel bars, spaced at 225 mm and arranged in the center of thickness. The bars were placed at about mid-thickness of the 50 mm slab, which gives a clear cover of about 20 mm to the nearest face for a centered Ø10 bar. Because the bars of the two directions cross, the two layers cannot both lie exactly at mid-thickness; the effective depth of about 25 mm used in the checks of Section 2.7 is therefore an approximation, and the exact elevation of each layer is not reported.

The second group consisted of seven slabs with dimensions of 650 mm x 1000 mm x 100 mm. This group was reinforced with five Ø10 deformed steel bars, spaced at 150 mm along the short side (650 mm) and five Ø10 deformed steel bars spaced at 225 mm along the long side (1000 mm), as shown in Figure 2.

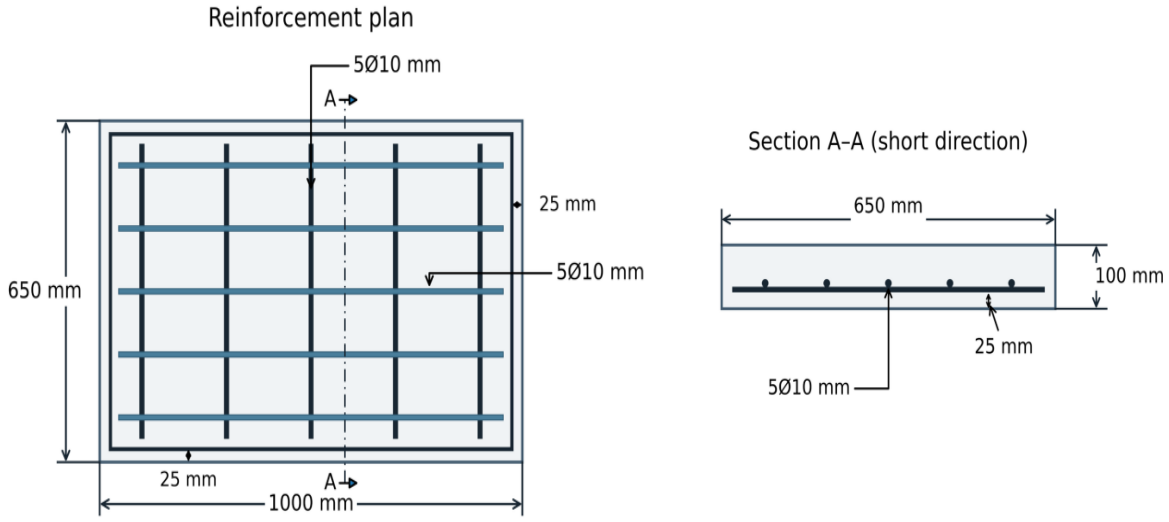


Fig. 2. Reinforcement details for the specimen of Group 2

Two slabs were constructed with normal steel reinforcement (CS-TH0-T0 and CS-TH50-T0). However, the difference lies in the coarse aggregate: The CS-TH0-T0 slab was constructed with normal coarse aggregate, whereas the CS-TH50-T0 slab incorporated recycled Thermostone as a 50% replacement of the coarse aggregate. The remaining slabs were also constructed with 50% Thermostone as a coarse aggregate replacement, but with varying replacement ratios for recycled tubes instead of the steel reinforcement specifically 20%, 40%, 60%, 80%, and 100%. This

replacement was defined by the number of tensile bars replaced (out of five per meter in each direction), applied in both the short-span and long-span directions: one bar replaced per direction corresponds to 20%, two to 40%, three to 60%, four to 80%, and all five to 100%. The details of the specimens for the first group are presented in Table 1, while those for the second group are presented in Table 2.

Table 1. Group 1 of the tested specimens

Specimen	Description
CS-GP0	Control slab without GP
CS-GP5	Slab with 5% GP replacement ratio
CS-GP10	Slab with 10% GP replacement ratio
CS-GP15	Slab with 15% GP replacement ratio
CS-GP20	Slab with 20% GP replacement ratio
CS-GP25	Slab with 25% GP replacement ratio

Table 2. Group 2 of the tested specimens

Specimen	Description
CS-TH0-T0	Slab with 0% of recycled Thermostone and reinforced with the steel reinforcement
CS-TH50-T0	Slab with 50% of recycled Thermostone and reinforced with the steel reinforcement
CS-TH50-T20	Slab with 50% of recycled Thermostone and 20% of the recycled tubes
CS-TH50-T40	Slab with 50% of recycled Thermostone and 40% of the recycled tubes
CS-TH50-T60	Slab with 50% of recycled Thermostone and 60% of the recycled tubes.
CS-TH50-T80	Slab with 50% of recycled Thermostone and 80% of the recycled tubes.
CS-TH50-T100	Slab with 50% of recycled Thermostone and 100% of the recycled tubes

2.2 Materials

Locally available materials were used to prepare all the tested specimens. Ordinary Portland cement complied with ASTM C150/C150M [20], Tikrit University network water with pH equal to 7.7, fine aggregate of 2.65 specific gravity, and crushed river gravel with a maximum aggregate size of 12 mm and 2.66 specific gravity. Both fine and coarse aggregates comply with [21,22].

2.3 Glass Powder

Glass powder (GP) can be considered a pozzolanic material, making it suitable for addition to concrete, cement paste, or mortar. Pozzolanic materials are synthetic substances consisting of active amorphous silica, which can develop bonding properties when interacting with calcium hydroxide ($Ca(OH)_2$) in the presence of water at normal temperatures. This pozzolanic reactivity of recycled glass powder has also been confirmed at the microstructural level in high-strength reactive powder concrete systems [23]. In the GP concrete used in this study, the glass aggregate was sourced from waste homemade glass bottles collected from local vendors. The glass was cleaned and crushed using the Los Angeles machine to a thickness of 2 mm. After collection, it was sifted to obtain particle sizes similar to those of natural fine aggregate, ensuring their gradation conformed to Iraqi standards. Particle-size distribution is a key control on the performance of recycled glass powder, since finer granularity generally enhances pozzolanic reactivity [24]. Details of the GP mix are shown in Table 3. The crushing of the waste glass and the resulting glass powder are shown in Figure 3. The glass powder was characterized as follows: SiO_2 72.8%, Na_2O 12.4%, specific gravity 2.61, Blaine fineness 4100 cm^2/g, and mean particle size 20 micron. Fresh- and hardened-state properties were also measured: slump = 80 mm; split-tensile strength = 6.37, 6.75, 6.58, and 6.42 MPa at 28 days for the 10%, 15%, 20%, and 25% glass-powder replacement ratios, respectively (a value for the 5% ratio was not separately measured).



Fig. 3. Crushing of the waste glass (left) and the resulting glass powder (right)

Table 3. Mix proportions/m3 for GP concrete

Specimen	Water kg/m³	Cement kg/m³	Coarse aggregate kg/m³	Sand kg/m³		w/c	Superplasticizer (kg/m³)
				Normal weight	Glass Waste		
CS-GP0	145	**345**	898	621	0	0.42	10.4
CS-GP5	130	350	898	590	31	0.37	10.5
CS-GP10	124	365	898	559	62	0.34	11.0
CS-GP15	120	376	898	528	93	0.32	11.3
CS-GP20	121	390	898	497	124	0.31	11.7
CS-GP25	120	400	898	466	155	0.30	12.0

2.4 Thermostone

The Thermostone used in Thermostone concrete is a building unit used in constructing walls for various buildings. This material is considered cheap compared to other building units. The aluminum powder is one of the Thermostone components to form cellular concrete and thus obtains a suitable density of (600 - 800) kg/m³, which is the secret of its light weight. Thermostone aggregate resulting from available construction waste was used in this study after crushing it manually using a hand hammer in multiple crushing stages (large pieces, then into smaller and smaller pieces) until a maximum nominal size of 12 mm was reached, Figure 4 shows the final sizes of the Thermostone. It was then sieved to ensure that the required gradation complies with coarse aggregate requirements. A water/cement ratio of 0.545 without superplasticizer, and of 0.39 with superplasticizer was used. Table 4 shows the mixes details.



Fig. 4. Thermostone final sizes

Table 4. Mix proportions/m3 for the second group of the slabs

Specimen	Water	Cement	Sand	Coarse aggregate	Thermostone	Tensile bars replaced by tubes
	kg/m³	kg/m³	kg/m³	kg/m³	kg/m³	%
CS-TH0-T0	**188**	345	837	**1225**	0	0
CS-TH50-T0	159	407	837	613	612	0
CS-TH50-T20	159	407	837	613	612	20
CS-TH50-T40	159	407	837	613	612	40
CS-TH50-T60	159	407	837	613	612	60
CS-TH50-T80	159	407	837	613	612	80
CS-TH50-T100	159	407	837	613	612	100

2.5 Hollow Tubes

The reinforcement consisted of steel bars with a diameter of 10 mm, a yield stress fy=350 MPa, and a steel area per direction of 392.7 mm^2 (five bars, Group 2) or 235.6 mm^2 (three bars, Group 1). Expressed per unit width, the bars at 150 mm spacing provide about 524 mm^2/m and those at 225 mm spacing about 349 mm^2/m; the number of bars in a slab is distinct from the steel area per metre width. The reinforcement ratio was determined using Method-III [25, 26]. Hollow iron pipes, with an external diameter of 18.75 mm and an internal diameter of 15.5 mm, were used to replace these bars. The annular steel cross-sectional area of the tube, calculated from the reported diameters as $\pi/4x(18.75^2\text{-}15.5^2) \approx 87.4$ mm^2, is about 11% larger than the 78.5 mm^2 cross-sectional area of the Ø10 bar it replaces; the two are therefore comparable but not exactly equal in steel area. The substitution was intended to match cross-sectional (steel) area as closely as practicable rather than yield force or flexural stiffness; the resulting ~11% area increase was accepted as the nearest available equivalence. This is shown in Figure 5. The recycled tube material was steel grade S355; its tensile properties, determined by tensile testing in accordance with ASTM A370 [27] and ASTM E8 [28], were a measured yield strength fy = 355 MPa, ultimate strength fu = 510 MPa, elastic modulus E = 210 GPa, and a nominal wall thickness of 1.625 mm (measured variation ±0.05 mm).

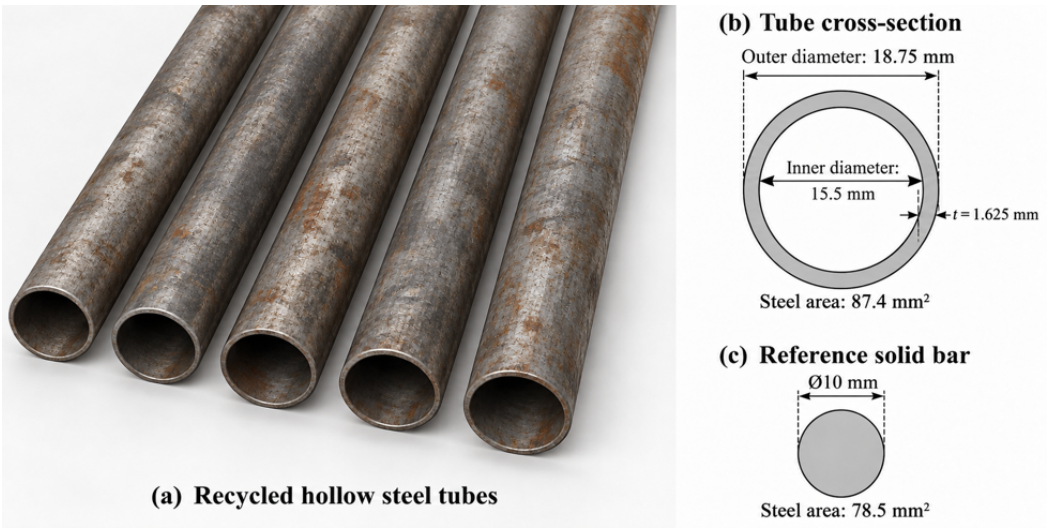


Fig. 5. Recycled hollow steel tubes: (a) illustrative view of the tubes; (b) tube cross-section; (c) reference Ø10 mm bar

The target compressive strength for the designed mix was 30 MPa, a normal-strength level chosen to represent common structural concrete so that the effect of the recycled materials could be judged against a conventional baseline. More than 30 mixtures with 3% cement weight superplasticizer (the same dosage was used for all Group 1 mixes, Table 3) were tested to obtain concrete with a strength equal to that of normal-weight concrete and a density of 1820 kg/m^3. To determine the compressive strength of each group, three specimens were tested.

2.6 Preparation of Specimens

The specimens were cast using iron molds for both groups of concrete specimens designated for this purpose, as shown in Figure 6. Before pouring, the molds were thoroughly cleaned and lightly oiled to prevent the hardened concrete from adhering to their interiors. All molds were filled with soft concrete and vibrated for one minute using electric vibrators. After vibration, the surfaces of the specimens were leveled with a trowel to obtain flat, numbered surfaces, and then covered with a nylon layer for 24 hours under lab conditions to prevent water evaporation and avoid cracks from plastic shrinkage. The specimens were then demolded and kept in water until the day of testing. The preparation for pouring the specimens is illustrated in Figure 6.



Fig. 6. Preparation for pouring the concrete

2.7 Instruments and Test Setup

All specimens were subjected to a concentrated load at the center of the specimen and tested using a Universal Testing Machine (SANS). A 2000 kN capacity of hydraulic jack and a loading rate of 1.75 kN/s was used to measure the applied loads in the middle of each slab up to failure. One vertical LVDT with a sensitivity of 0.001 mm was placed below the specimen to record the vertical deflection at the slab center. The measurement data were collected at fixed intervals by using a computer-controlled data acquisition system. Only a single LVDT, placed at the slab center, was used; no LVDTs were placed at the supports, so the deflections reported are the absolute central deflections and no correction for support settlement was applied (see Figure 8A). The load was applied directly through the hydraulic jack ram as a concentrated (point) load at the slab center, with no separate loading plate used to distribute it over a larger bearing area. The loading bearing-contact area was circular with a diameter of 115 mm, the support width was 40 mm, and the clear span between the inner edges of the supports was 450 mm in both directions (about 490 mm center-to-center for the 40 mm-wide supports), for both slab groups. The slabs were simply supported on these supports. A preliminary two-way (punching) shear check was carried out using the simplified ACI 318 [25] expression $V_c = 0.33\lambda\sqrt{f'_c}\cdot b_0\cdot d$, with the critical perimeter $b_0 = \pi(a + d)$ taken at $d/2$ from the 115 mm loaded circular area, $\lambda = 1.0$, and d (effective depth to the tension-steel centroid) taken as ≈25 mm for the 50 mm-thick Group 1 slabs (consistent with the near-mid-thickness bar placement reported above) and ≈70 mm for the 100 mm-thick Group 2 slabs (25 mm cover, 10 mm bars). For Group 2, the resulting estimated nominal capacity (≈73.5 kN, computed with the 30 MPa target strength because the measured Group 2-cylinder strengths are not tabulated in this paper) is roughly 2–5 times the observed peak loads (15–37 kN), so punching shear is not expected to govern, consistent with the flexural failure mode observed for all specimens. For Group 1, however, the same simplified check gives an estimated nominal capacity of only about 14–20 kN (depending on each mix's measured f'c, Table 5), which is below the observed peak loads of 19–28 kN for every specimen in this group — yet the failure mode physically observed and documented for all Group 1 specimens (cracking initiating at the slab

center and propagating outward; see Figure 9) was flexural, not a punching cone. Because the ACI 318 expression used here is a conservative design-oriented lower bound rather than a best-estimate predictor, and because of residual uncertainty in the true effective depth for these very thin (50 mm) slabs and in the actual bearing geometry of the jack ram, this numerical shortfall should be read as indicative rather than as evidence against the observed flexural failure mode. It is reported here transparently and is tentatively attributed to these conservatisms, including the size effect, which is known to raise the apparent shear capacity of thin slabs above code predictions calibrated on thicker members; it could not be verified further because only the applied load and the central deflection were instrumented. A local-crushing (bearing) check was also carried out per ACI 318, using $P_n = 0.85f'_c \cdot A_1$ (unconfined, a lower bound; confinement from the surrounding slab could permit up to $2 \times 0.85f'_c \cdot A_1$) with $A_1 = 10{,}387$ mm^2 (the 115 mm-diameter loaded area). This gives an estimated nominal bearing capacity of about 136–262 kN for Group 1 (across its range of measured f'c) and about 265 kN for Group 2 (at the 30 MPa target strength), both far above the observed peak loads (19–28 kN and 15–37 kN, respectively); local crushing under the loaded area is therefore not expected to govern for either group. A one-way (beam) shear check was also carried out according to ACI 318, using $V_c = 0.17\lambda\sqrt{f'_c} \cdot b \cdot d$ with b = 450 mm (the clear span width) and the same effective depths as above, conservatively assuming that the entire applied load P is carried in a single direction, so that the shear at each support is P/2. For Group 2 the estimated capacity (≈29.3 kN at the 30 MPa target strength) exceeds the maximum support shear (18.5 kN, specimen CS-TH0-T0) by a factor of at least 1.6. For Group 1 the capacity is about 7.5–10.4 kN (depending on each mix's f'c), which is below the support shear of 9.5–14 kN under this single-direction idealization; however, for a slab supported along its edges in both directions the load is shared between the two directions, the shear per direction is about P/4 (4.8–7.0 kN), and the capacity then exceeds it by a factor of about 1.4–1.6. One-way shear is therefore not expected to govern for either group, consistent with the observed flexural failure, although the margin for Group 1 is small. Figure 7 shows the test setup used for all the specimens.



Fig. 7. Test setup

3. Results and Discussion

3.1 Performance of the First Group of Slabs

3.1.1 Load-Deflection Behavior

The load-deflection behavior of the specimens constructed with different ratios of glass powder is depicted in Figure 8A. The central deflection shown in the figure represents the deflection recorded at the center of the slab by the single center-point LVDT. Only a single LVDT at the slab center was used, so the deflection distribution over the slab was not measured and the location of the maximum deflection cannot be established from these data (the test setup is shown in Figure 7).

Following meticulous testing and preparation, the control specimen constructed without GP (CS-GP0) reached an ultimate load of 28 kN at a deflection of 5.33 mm. The specimen with 5% GP (CS-GP5) reached an ultimate load only about 3.6% below the control, confirming that low glass-powder content does not compromise load capacity; however, its deflection at peak load (5.97 mm) was about 12% higher than the control, rather than lower, so the two responses (load and deflection) should not be assumed to change in the same direction. Increasing the amount of glass powder in the concrete led to a decrease in the ultimate load. Table 5 represents a summary of the ultimate loads and deflections for all the specimens.

Table 5. Summary of test results for the specimens with recycled GP

Specimen	f'_c	Peak load	Deflection at peak load	f'c/f'c,control	Δpeak/Δpeak,control
	MPa	kN	mm	-	-
CS-GP0	29.7	28	5.33	-	-
CS-GP5	26.0	27	5.97	0.87	1.12
CS-GP10	22.7	25	5.37	0.76	1.01
CS-GP15	19.9	24	5.30	0.67	0.99
CS-GP20	17.2	22	5.56	0.58	1.04
CS-GP25	15.4	19	5.60	0.52	1.05

In Table 5, the two rightmost columns express, respectively, the ratio of each mix's compressive strength to that of the control (f'c/f'c,control) and the ratio of its deflection at peak load to that of the control (Δpeak/Δpeak,control); values below 1.0 indicate a reduction relative to CS-GP0. These ratios are consistent with the tabulated f'c and deflection values for all specimens. The f'c/f'c,control ratio for CS-GP20 is 0.58 (17.2/29.7), consistent with the 17.2 MPa compressive strength of that mix.

Comparison with previous work: the decline in ultimate load with increasing glass-powder content contrasts with the optimum replacement of about 20% reported by Prema Kumar et al. [5] and by Nwofor and Ukpaka [8]. However, those studies replaced cement, or coarse and fine aggregates, under different conditions, and in the present slabs the cement content and w/c ratio also varied between mixes, so the results are not directly comparable. The small loss of capacity at 5% replacement (about 3.6%) is consistent with the acceptable behavior at moderate replacement ratios reported for glass-containing beams by Mustafa et al. [17].

3.2 Performance of The Second Group of Slabs

3.2.1 Load-Deflection Behavior

The load-deflection relationship for the specimens that are reinforced with different ratios of the recycled tube is presented in Figure 8B and summarized in Table 6, using the original test data. The unmodified control specimen CS-TH0-T0 reached the highest peak load, 37 kN, at a deflection of 25 mm. Peak load then decreased progressively with increasing recycled-tube replacement: 35 kN for CS-TH50-T0 (the 0%-replacement, 50%-Thermostone reference), 30 kN for both CS-TH50-T20 and CS-TH50-T40, 25 kN for CS-TH50-T60, 20 kN for CS-TH50-T80, and 15 kN for CS-TH50-T100 — a reduction of 59.5% relative to the control at full replacement, or 57.1% relative to the CS-TH50-T0 reference (35 kN), which isolates the effect of the tubes from that of Thermostone. This indicates that, unlike Group 1, the recycled tubes reduce the load-bearing capacity of Group 2 specimens progressively across the whole tested range, rather than only beyond a threshold. The deflection at peak load stayed in a comparatively narrow band across specimens (17.7–25 mm), without a clear, monotonic ductility increase; CS-TH50-T40 (20 mm) and CS-TH50-T100 (17.7 mm) in particular reached peak load at a smaller deflection than the control, so the recycled tubes should not be described as uniformly enhancing ductility over this range.

Values are the point-by-point load-deflection test data for all seven Group 2 specimens (Figure 8B); change in peak load is expressed relative to the unmodified control CS-TH0-T0 (37 kN). Peak load decreases progressively with increasing recycled-tube replacement ratio, from 37 kN (control) to 15 kN at 100% replacement, a reduction of 59.5%; relative to the 50%-Thermostone reference (35

kN), the tubes alone account for a reduction of 57.1%. The ductility index μ is defined below; "≥" marks a lower bound.

Table 6. Summary of test results for the specimens with recycled tubes

Specimen	Peak load (kN)	Deflection at peak load (mm)	Change in peak load vs. control (%)	Ductility index μ
CS-TH0-T0	37	25	0	≥ 1.26
CS-TH50-T0	35	24	-5	≥ 1.26
CS-TH50-T20	30	24	-19	≥ 1.32
CS-TH50-T40	30	20	-19	≥ 1.71
CS-TH50-T60	25	24	-32	1.43
CS-TH50-T80	20	24	-46	1.17
CS-TH50-T100	15	17.7	-59	≥ 1.45

Ductility was quantified with the displacement ductility index $\mu = \Delta u/\Delta y$, where $\Delta y = \Delta 0.75/0.75$ is the equivalent yield deflection ($\Delta 0.75$ being the deflection at 75% of the peak load on the ascending branch, after Park [29]) and Δu is the deflection at which the load falls to 85% of the peak load on the descending branch, or the last recorded deflection when the load did not fall to 85% of the peak, in which case μ is a lower bound (marked ≥). The Group 2 values are given in Table 6: μ ranged from 1.17 to 1.71 with no consistent trend with the tube-replacement ratio, and the controls CS-TH0-T0 and CS-TH50-T0 (both ≥ 1.26) fall within this range, so the data do not demonstrate ductility enhancement. For Group 1, μ was ≥ 1.18 (CS-GP0), ≥ 1.27 (CS-GP5), ≥ 1.20 (CS-GP10), ≥ 1.27 (CS-GP15), ≥ 1.28 (CS-GP20) and ≥ 1.49 (CS-GP25). Because most values are lower bounds (≥), the true indices may be higher, so no conclusion on absolute ductility is drawn; the data show no clear trend of ductility enhancement with tube replacement. The 85% post-peak load level follows the common definition of the ultimate deflection as the point at which the load has dropped by 15% from its peak, after Park [29]; the curves were recorded at coarse load increments, so the indices are indicative.

Comparison with previous work: the progressive decrease in peak load with tube replacement agrees with the reductions in ultimate load reported by Al-Bayati et al. [19] for slabs with hollows, but differs from the insignificant change in capacity reported by Rajeshwaran et al. [11] for hollow pipes. Because the steel area (87.4 mm^2 against 78.5 mm^2) and yield strength (355 MPa against 350 MPa) of the tubes are not lower than those of the bars they replace, the reduction in capacity may reflect the tube–concrete separation observed at failure (bond or anchorage loss) rather than a lack of steel; this could not be confirmed without a dedicated bond test.

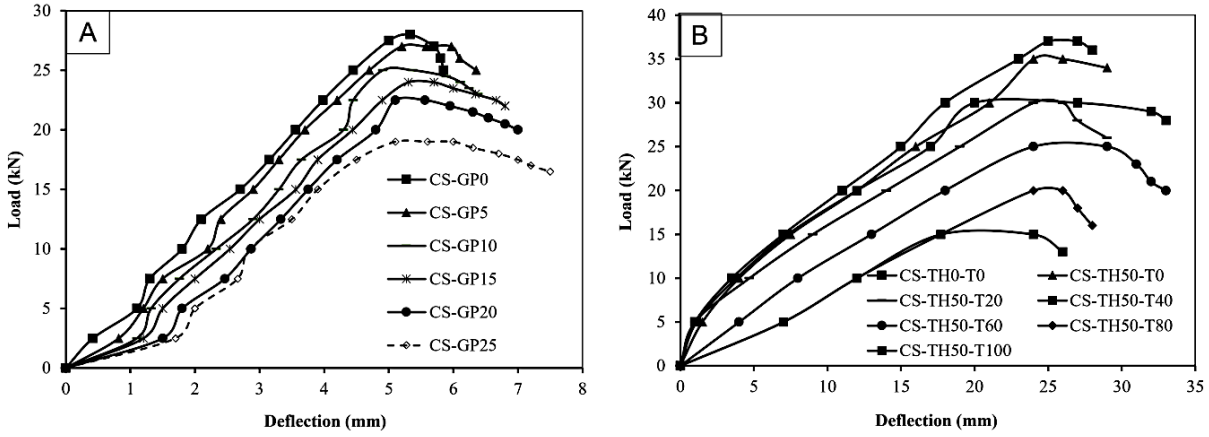


Fig. 8. A. Load-deflection relationship for the specimens with GP; B. Load-deflection behavior of the specimens with different ratios of the recycled tubes

Note that the deflection-axis range differs between panels A and B because the two groups used different slab dimensions (500 × 500 × 50 mm for Group 1 versus 650 × 1000 × 100 mm for Group 2), not a plotting inconsistency.

3.3 Failure Modes

The failure mode for all specimens was a flexural failure. The failure began with weak cracks in the area close to the supports. They grew gradually and spread over the whole area until the specimen failed. For the recycled tubes, it was seen that they were separated from the concrete and bent. Figure 9 shows the crack distribution on the tension surface and failure modes for the specimens with the GP. For all the tested specimens, cracks started on the bottom surface of the slab (tension side) at the loading point (center of the slab) and propagated towards the slab extremities with increasing load.

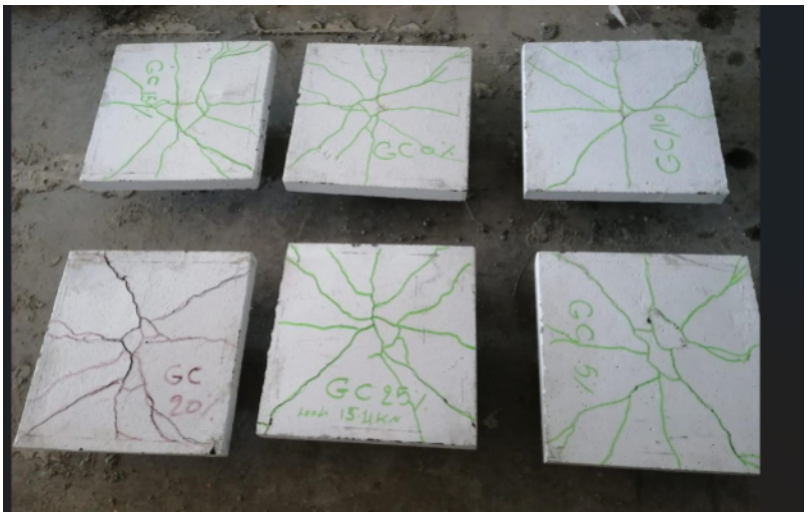


Fig. 9. Failure mode for the specimens with different GP ratios

3.4 Environmental and Material-Flow Assessment

Beyond structural performance, the mix data in Table 3 and Table 4 allow a first-order estimate of the material and carbon implications of the two recycling strategies. Using the global average emission intensity of ordinary Portland cement of approximately 0.673 kg CO2e per kg [30], the cement-related embodied carbon of the GP mixes rises from about 232 kg CO2e/m^3 for the control mix (345 kg/m^3 cement) to about 262 kg CO2e/m^3 at 20% GP replacement (390 kg/m^3 cement), an increase of roughly 13%. This indicates that, although each cubic meter of GP concrete diverts 124 kg of waste glass at 20% replacement (up to 155 kg at 25%) and reduces natural sand demand by the same amount, the associated rise in cement content required to maintain workability and strength partially offsets the environmental benefit of aggregate substitution. This trade-off, driven by cement dominating the carbon footprint of concrete regardless of aggregate source [31], should be weighed explicitly in any sustainability claim made for the GP mixes. For the second group, the 50% Thermostone replacement reduces the natural coarse aggregate from 1225 to 613 kg/m^3 (612 kg/m^3 replaced), but Table 4 also shows the cement content rising from 345 to 407 kg/m^3 (+62 kg/m^3, about 18%), which with the same emission factor raises the cement-related embodied carbon from about 232 to about 274 kg CO2e/m^3. The material-flow benefit of Thermostone is therefore partly offset by the extra cement, as for the glass-powder mixes, and its net benefit cannot be stated without the embodied carbon of the Thermostone itself. A full life-cycle assessment, including transport and processing emissions of the recycled glass and Thermostone, is recommended as a direct extension of this work before quantitative sustainability claims are generalized.

3.5 Limitations and Future Work

Two limitations should be acknowledged. First, each mix configuration in both groups was represented by a single structural slab specimen; while three companion cylinders were used to characterize compressive strength, the structural load-deflection results reported here were not statistically replicated, and the reported trends should be interpreted as indicative rather than as population estimates. Second, the experimental results were not benchmarked against a theoretical or numerical prediction (e.g., yield-line theory or a finite-element model); such a comparison would

strengthen confidence in the reported capacities and is recommended as the next step before these findings are generalized to design practice.

4. Conclusions

This study tested thirteen reinforced concrete two-way slabs in two groups under a monotonic central load; each configuration being represented by a single specimen. In Group 1, replacing fine aggregate with waste glass powder (GP) lowered the ultimate load progressively: 5% GP reduced it by only about 3.6% relative to the control (28 kN), whereas 25% GP reduced it by about 32%. Compressive strength fell in parallel, but the cement content and the water/cement ratio also changed across the mixes, so the strength trend cannot be attributed to the glass content alone. Deflection was measured at the slab center with a single LVDT, so its distribution over the slab is unknown. In Group 2, replacing the tensile bars with recycled hollow steel tubes in slabs containing 50% Thermostone reduced the peak load progressively, from 37 kN for the control and 35 kN for the 50%-Thermostone reference to 15 kN at full replacement, that is, by 59.5% and 57.1%, respectively. Neither the deflection at peak load nor the displacement ductility index (1.2–1.7, mostly lower bounds) showed a clear ductility enhancement. Tube–concrete separation was observed at failure, so bond or anchorage loss may contribute to the capacity reduction, although this was not verified. These results agree with the reductions in capacity reported for slabs with hollows [19] and with the acceptable behavior at moderate glass replacement reported for beams [17]; the optimum glass-powder content of about 20% reported in [5] and [8] was not reproduced, probably because those studies replaced cement or used different aggregates and mixes. In practice, glass powder should be limited to low replacement ratios, and the loss of load capacity with tube replacement must be considered in design. Because of the single specimen per configuration, the findings are indicative; replicated tests, bond tests on the tubes and a comparison with a mechanics-based prediction are recommended before design use.

References

[1] Khanghahi SH, Hadidi MR, Mohammadi Y. Laboratory investigations on fracture toughness of self-compacting concrete containing recycled materials. Jordan Journal of Civil Engineering. 2024;18(2). https://doi.org/10.14525/JJCE.v18i2.03

[2] Abdelli HE, Mokrani L, Kennouche S, de Aguiar JLB. Utilization of waste glass in the improvement of concrete performance: a mini review. Waste Management & Research. 2020;38(11):1204-13. https://doi.org/10.1177/0734242X20941090

[3] Afshinnia K. Investigation into mechanisms and mitigation of alkali-silica reaction in sustainable Portland cement concrete containing recycled glass materials [PhD thesis]. Clemson (SC): Clemson University; 2015.

[4] Lee G, Ling TC, Wong YL, Poon CS. Effects of crushed glass cullet sizes, casting methods and pozzolanic materials on ASR of concrete blocks. Construction and Building Materials. 2011;25(5):2611-8. https://doi.org/10.1016/j.conbuildmat.2010.12.008

[5] Prema Kumar WP, Ananthayya MB, Vijay K. Effect of partial replacement of cement with waste glass powder on the properties of concrete. International Journal of Structural and Civil Engineering Research. 2014;3:1-6.

[6] Liaqat M, Shah ML, Baig MA. Effect of waste glass as partial replacement for coarse aggregate in concrete. International Journal of Technical Innovation in Modern Engineering & Science. 2018;4(6):609-19.

[7] Jomaa'h MM. Effect of lightweight coarse aggregate from claystone and thermostone on physical and mechanical properties of concrete. Diyala Journal of Engineering Sciences. 2017;10(1):1-17. https://doi.org/10.24237/djes.2017.10301

[8] Nwofor TC, Ukpaka C. Predictive models for compressive strength of concrete produced with waste glass as replacement for aggregates. International Journal of Civil Engineering. 2017;4(1):31-4. https://doi.org/10.14445/23488352/IJCE-V4I1P104

[9] Klak FS, Tais AS, Al-Hadithy LK. Properties of conventional concrete containing waste glass powder. AIP Conference Proceedings. 2024;2864. https://doi.org/10.1063/5.0186117

[10] Gamal AA. Strengthening techniques in reinforced concrete hollow core. International Journal of Engineering and Innovative Technology. 2015;4(8):159-73.

[11] Rajeshwaran R, Yamini V, Nivedha DGS, Madhu Bala AM. Experimental evaluation of concrete slab using hollow steel pipes. Civil Engineering Research Journal. 2018;5(4):161-4. https://doi.org/10.19080/CERJ.2018.05.555670

[12] Klak FS, Jomaa'h M, Ahmad S. Behavior of reinforced concrete members exposed to fire. Tikrit Journal of Engineering Sciences. 2022;29(4):56-68. https://doi.org/10.25130/tjes.29.4.7
[13] Newman J, Choo BS. Advanced concrete technology 3: processes. Oxford: Elsevier; 2003. https://doi.org/10.1016/B978-075065686-3/50288-3
[14] Abdulah MD. Behavior of reinforced lightweight concrete two way slabs strengthened with CFRP sheets. Engineering and Technology Journal. 2015;33(8A):1813-29. https://doi.org/10.30684/etj.2015.108825
[15] Zaher AA, Abdelrahman AA, Eldeib AS, Mohamed AA. Punching shear behavior of lightweight foamed RC slabs. International Journal of Application or Innovation in Engineering & Management. 2015;4(7):67-73.
[16] Klak FS, Jomaa'h MM. Conventional and lightweight aggregate one-way reinforced concrete slabs subjected to fire and repeated loads: comparative experimental study. Australian Journal of Structural Engineering. 2024;25(1):106-23. https://doi.org/10.1080/13287982.2023.2213504
[17] Mustafa TS, El Beshlawy SA, Nassem AR. Experimental study on the behavior of RC beams containing recycled glass. Construction and Building Materials. 2022;344:128250. https://doi.org/10.1016/j.conbuildmat.2022.128250
[18] Elsayed M, Abd-Allah SR, Said M, Abdel El-Azim A. Structural performance of recycled coarse aggregate concrete beams containing waste glass powder and waste aluminum fibers. Case Studies in Construction Materials. 2023;18:e01751. https://doi.org/10.1016/j.cscm.2022.e01751
[19] Al-Bayati J, Abuzaid EKM, Mohammed MH. Flexural behavior of reinforced concrete one-way slabs with longitudinal hollows. Journal of Engineering and Sustainable Development. 2024;28(5). https://doi.org/10.31272/jeasd.28.5.2
[20] ASTM C150/C150M-17. Standard specification for Portland cement. West Conshohocken (PA): ASTM International; 2017.
[21] ASTM C33-03. Standard specification for concrete aggregates. West Conshohocken (PA): ASTM International; 2003.
[22] ASTM C330-05. Standard specification for lightweight aggregates for structural concrete. West Conshohocken (PA): ASTM International; 2005.
[23] Hussain ZA, Aljalawi NMF. Behavior of reactive powder concrete containing recycled glass powder reinforced by steel fiber. Journal of the Mechanical Behavior of Materials. 2022;31(1):233-9. https://doi.org/10.1515/jmbm-2022-0025
[24] Younsi A, Mahi MA, Hamami AEA, Belarbi R, Bastidas-Arteaga E. High-volume recycled waste glass powder cement-based materials: role of glass powder granularity. Buildings. 2023;13(7):1783. https://doi.org/10.3390/buildings13071783
[25] ACI Committee 318. Building code requirements for structural concrete (ACI 318-14) and commentary. Farmington Hills (MI): American Concrete Institute; 2014.
[26] Nilson AH, Winter G. Design of concrete structures. 11th ed. New York: McGraw-Hill; 1991.
[27] ASTM A370-22. Standard test methods and definitions for mechanical testing of steel products. West Conshohocken (PA): ASTM International; 2022.
[28] ASTM E8/E8M-22. Standard test methods for tension testing of metallic materials. West Conshohocken (PA): ASTM International; 2022.
[29] Park R. Evaluation of ductility of structures and structural assemblages from laboratory testing. Bulletin of the New Zealand National Society for Earthquake Engineering. 1989;22(3):155-66. https://doi.org/10.5459/bnzsee.22.3.155-166
[30] International Renewable Energy Agency (IRENA). Decarbonising hard-to-abate sectors with renewables: enablers and recommendations, section 2.6 Cement [Internet]. Abu Dhabi: IRENA; 2025 [cited 2026 Oct 13]. Available from: https://www.irena.org/Decarbonising-hard-to-abate-sectors-with-renewables-Enablers-and-recommendations/Industry-sector/Cement
[31] Jiménez LF, et al. Carbon footprint of recycled aggregate concrete. Advances in Civil Engineering. 2018;2018:7949741. https://doi.org/10.1155/2018/7949741